Molecular Therapy
Nucleic Acids
Original Article

Enhancement of myogenic differentiation and inhibition of rhabdomyosarcoma progression by miR-28-3p and miR-193a-5p regulated by SNAIL

Klaudia Skrzypek,[1] Artur Nieszporek,[1] Bogna Badyra,[1] Małgorzata Lasota,[1] and Marcin Majka[1]

[1]Jagiellonian University Medical College, Faculty of Medicine, Institute of Pediatrics, Department of Transplantation, Wielicka 265, 30-663 Krakow, Poland

Rhabdomyosarcoma (RMS) is a soft tissue mesenchymal tumor that affects mostly children and adolescents. It originates from the impaired myogenic differentiation of stem cells or early progenitors. SNAIL, a transcription factor that regulates epithelial-to-mesenchymal transition in tumors of epithelial origin, is also a key regulator of RMS growth, progression, and myogenic differentiation. Here, we demonstrate that the SNAIL-dependent microRNAs (miRNAs) miR-28-3p and miR-193a-5p are crucial regulators of RMS growth, differentiation, and progression. miR-28-3p and miR-193a-5p diminished proliferation and arrested RMS cells in G0/G1 phase *in vitro*. They induced the myogenic differentiation of both RMS cells and human myoblasts by upregulating myogenic factors. Furthermore, miR-28-3p and miR-193a-5p inhibited migration in a scratch assay, adhesion to endothelial cells, chemotaxis, and invasion toward SDF-1 and HGF and regulated angiogenic capabilities of the cells. Overexpression of miR-28-3p and miR-193a-5p induced formation of fibrotic structures and abnormal blood vessels in RMS xenografts in immunodeficient mice *in vivo*. Simultaneous overexpression of both miRNAs diminished tumor growth after subcutaneous implantation and inhibited the engraftment of RMS cells into bone marrow after intravenous injection *in vivo*. To conclude, we discovered novel SNAIL-dependent miRNAs that may become new therapeutic targets in RMS in the future.

INTRODUCTION

Rhabdomyosarcoma (RMS) is one of the most common mesenchymal soft tissue tumors among children and adolescents. RMS origin is associated with the myogenic differentiation defect of stem cells or early progenitors.[1] Although RMS cells express muscle differentiation markers, these tumors do not fully differentiate.[1] Two main RMS subtypes are distinguished based on the histological analysis of tumors, embryonal RMS (ERMS) and alveolar RMS (ARMS), which usually displays a significantly poor prognosis due to the presence of *PAX3/7-FOXO1* fusion gene[2] and increased levels of tyrosine receptor kinases,[1] such as FGFR4 (fibroblast growth factor receptor 4) or IGF1R (insulin-like growth factor 1 receptor)[3] and MET receptor.[4,5] The main obstacle in patient survival is the metastatic process. The overall survival rate at 3 years is only 25%–30% in patients with high-grade tumors with metastatic involvement.[1] Understanding the mechanisms of tumor development, local invasion, and metastasis is necessary for the development of novel therapeutics in the future.

The SNAIL (SNAI1) transcription factor is one of the crucial regulators of ARMS growth.[6] SNAIL is a zinc finger transcription factor that usually acts as a gene repressor by binding to E-box sequences in promoters of genes and thus regulates epithelial-to-mesenchymal transition in epithelial cancer progression.[7,8] SNAIL levels are elevated in ARMS[6,9] and increase with tumor stage.[6] SNAIL silencing completely abolishes the growth of human ARMS xenotransplants[6] because SNAIL affects myogenic differentiation and the expression or activity of myogenic factors.[6,10] Furthermore, SNAIL regulates RMS metastasis by affecting the EZRIN cytoskeletal protein and AKT serine/threonine kinase levels.[11] In addition to the regulation of protein expression, SNAIL is also a crucial regulator of noncoding RNAs, including microRNAs (miRNAs).[7,11] SNAIL may affect miRNA expression either indirectly or directly by binding to their promoters or regulatory elements.[7] In our previous studies, we demonstrated that in RMS cells SNAIL is the regulator of the whole miRNA transcriptome, and gene ontology analysis revealed that the SNAIL-miRNA axis regulates processes associated with differentiation, migration, and reorganization of the actin cytoskeleton.[11] Furthermore, we selected miRNAs that were the most potently regulated by SNAIL for further investigation of their effects on RMS migration. Two of the candidates, miR-28-3p and miR-193a-5p, regulated the motility of RMS cells after transient transfection with miRNA mimics,[11] but their precise modes of action have not been described.

miR-193 family members act as tumor suppressors in many tumor types, and miR-193a-3p is considered the main strand that is the most described in many tumor types.[12] Nevertheless, the role of

Received 25 September 2020; accepted 13 April 2021;
https://doi.org/10.1016/j.omtn.2021.04.013.

Correspondence: Marcin Majka, PhD, DSc, Jagiellonian University Medical College, Faculty of Medicine, Institute of Pediatrics, Department of Transplantation, Wielicka 265, 30-663 Krakow, Poland.
E-mail: mmajka@cm-uj.krakow.pl
Correspondence: Klaudia Skrzypek, PhD, Jagiellonian University Medical College, Faculty of Medicine, Institute of Pediatrics, Department of Transplantation, Wielicka 265, 30-663 Krakow, Poland.
E-mail: klaudia.skrzypek@uj.edu.pl

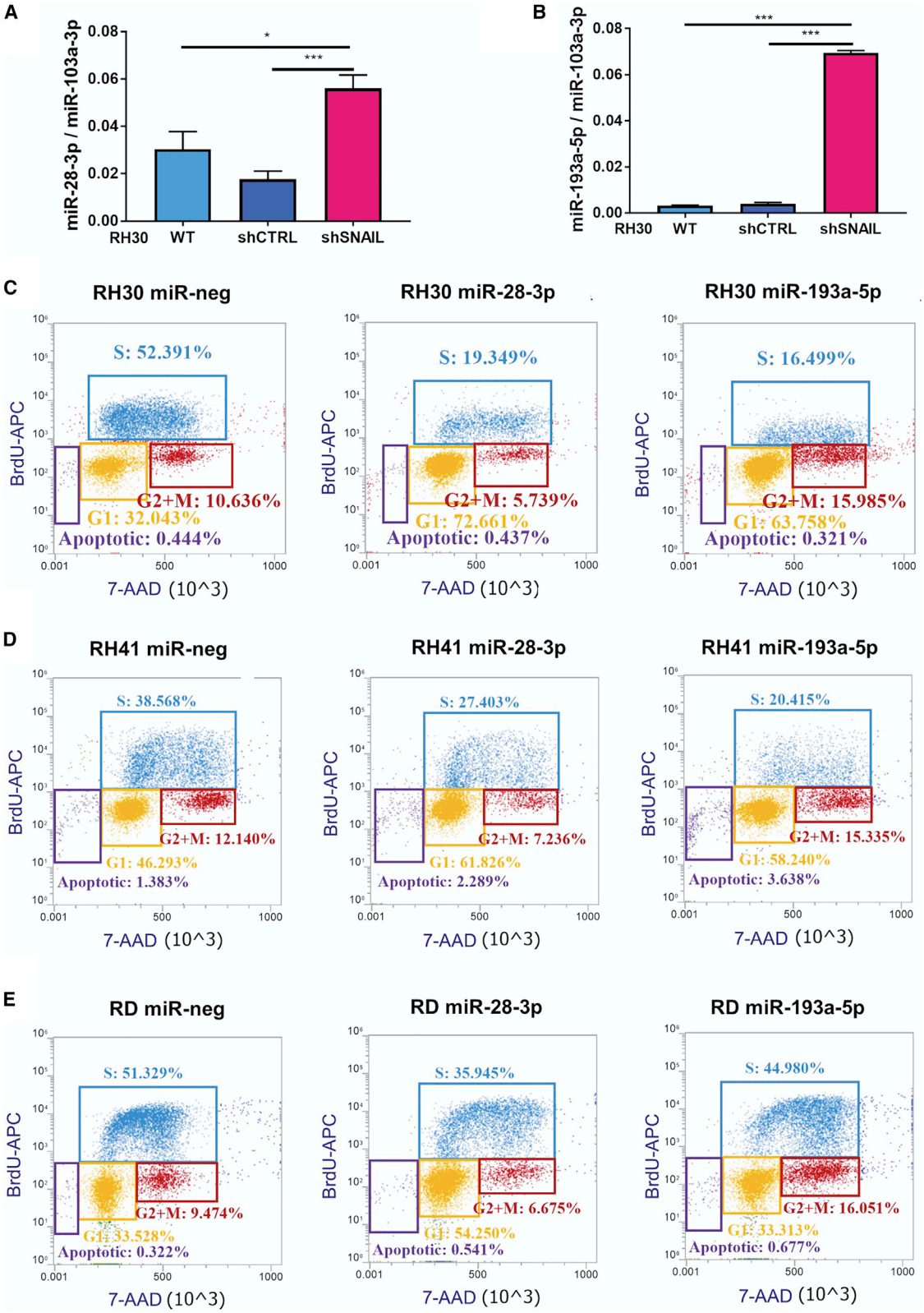

(legend on next page)

miR-193a-5p in tumor progression is also crucial. miR-193a-5p inhibits the migratory capabilities of colon cancer cells and suppresses the metastasis pathway.[13] Its important role was also described in endometrial adenocarcinoma[14] and osteosarcoma.[15] miR-28 is also an important regulator of tumor growth. miR-28 is regulated by STAT5 and p53 binding to its promoter,[16] which suggests that it may play a crucial role in tumor development. miR-28-5p is mostly described in many tumor types and is considered as the main strand. Nevertheless, the effects of the second strand (miR-28-3p) were also described in tumors. Surprisingly, miR-28-3p and miR-28-5p have distinct effects on colorectal cancer cells.[17] Studies have suggested that miR-28-3p may be involved in the phosphatidylinositol signaling pathway, which is important in many tumors.[18]

The roles of several miRNAs in RMS growth and progression have already been described. Some of them, such as miR-410-3p or miR-874, inhibit migratory capabilities of the cells.[19,20] The most widely described group involves miRNAs that can inhibit tumor growth by promoting myogenic differentiation, such as miR-206,[21] miR-450b-5p,[22] miR-29,[23] and miR-411-5p.[24] Nevertheless, further studies on miRNAs in RMS are still required.

Interestingly, miR-28 and miR-193a are upregulated in differentiating myoblasts, which suggests their potential roles in myogenic differentiation.[25] Furthermore, our previous studies suggested important roles of SNAIL-dependent miR-28-3p and miR-193a-5p in the regulation of RMS migration.[11] Therefore, in this study we evaluated the roles of miR-28-3p and miR-193a-5p in RMS growth, differentiation, vascularization, and metastasis. We found that miR-28-3p and miR-193a-5p are crucial mediators of SNAIL action and important targets for future therapies.

RESULTS

SNAIL-regulated miR-28-3p and miR-193a-5p affect proliferation of RMS cells

Recently, we demonstrated by next-generation sequencing (NGS) that the SNAIL transcription factor is a crucial regulator of the miRNA transcriptome in RMS.[11] Here, we validated by qPCR the expression levels of the two candidate miRNAs that were among the most potently upregulated in SNAIL-deficient RH30 cells (shSNAIL). miR-28-3p (Figure 1A) and miR-193a-5p (Figure 1B) were significantly upregulated in RH30 shSNAIL cells compared with scrambled short hairpin RNA (shRNA) (shCTRL) and wild-type (WT) cells. Chromatin immunoprecipitation sequencing (ChIP-seq) analysis, performed previously (data were deposited into the Gene Expression Omnibus (GEO) database under GEO: GSE152355),[11] helped us to investigate whether miR-28-3p or miR-193a-5p is regulated by direct binding of the SNAIL transcription factors to the regulatory regions of their genes. ChIP-seq did not reveal any binding sites in the miR-28-3p or miR-193a-5p genes or their regulatory regions that differed significantly between immunoprecipitated and input samples,[11] which might suggest that SNAIL regulates their expression indirectly. Nevertheless, regulatory regions of MIR28 (Figure S1) and MIR193A (Figure S2) were also analyzed with Integrative Genomics Viewer (IGV). These regions involved 1,000 bp fragments upstream of the MIR28 and MIR193A genes, as well as the *LPP* (LIM domain containing preferred translocation partner in lipoma) promoter, the host gene for MIR28.[16] There was a slight tendency for an enhanced signal in samples immunoprecipitated with the anti-SNAIL antibody in regulatory regions of the MIR193A gene rather than the MIR28 gene (Figures S1 and S2), but those differences were not statistically significant in previous analyses.[11] Nevertheless, new significant SNAIL binding sites were discovered via ChIP-seq analysis (Figure S3). SNAIL bound to the intron of MIR193BHG, as well as to promoter-TSS (transcription start site) regions of the MIR3191 and MIR8072 genes (data were deposited into GEO: GSE152355,[11] and IGV results are shown in Figure S3). miR-3191 and miR-8072 expression was not previously detected in RH30 cells via NGS, but miR-193b was expressed and upregulated in SNAIL-deficient RH30 cells (for miR-193b-5p: logFC (log fold change) = 1.66, p = 1.93E−13; for miR-193b-3p: logFC = 1.73, p = 4.75E−09 compared with shSNAIL versus shCTRL) (data were deposited into GEO: GSE100114).[11] Interestingly, the SNAIL binding site in the intron of the MIR193BHG gene harbors regulatory enhancer feature ENSR00000531872 and partially ENSR00000083669 according to the Ensembl database (human GRCh38.p13).[26]

Since the aim of the study was to investigate the precise role of the SNAIL-dependent miRNAs miR-28-3p and miR-193a-5p in RMS development and metastasis, their expression levels were stably upregulated in RH30 cells by transduction with lentiviral vectors and transiently upregulated by transfection with miRNA mimics in RH41 and RD cells, as different techniques regulating expression levels help to discover biologically significant results. Control cells were modified with scrambled, nontargeting miRNA sequences (miR-neg) (Figures S4A and S4B). These modifications were strand specific and did not upregulate the second strand levels of miR-28-5p (Figure S4C) and miR-193a-3p (Figure S4D) in RH30 cells. Interestingly, miR-193a-5p overexpression in RH30 cells tended to upregulate a known myogenic-related miRNA, miR-206 (Figure S4E). Subsequently, we evaluated whether miR-28-3p and miR-193a-5p back-regulate SNAIL protein levels in RH30 (Figure S4F) and RH41 (Figure S4G) cells, but no significant effects were visible. miR-28-3p and miR-193a-5p overexpression induced an elongated phenotype of RH30 and RH41 cells

Figure 1. SNAIL-regulated miR-28-3p and miR-193a-5p affected the proliferation of RMS cells

(A and B) miR-28-3p (A) and miR-193a-5p (B) were upregulated in SNAIL-deficient RH30 cells (shSNAIL); n = 3–4. qPCR results were calculated with the ΔCt method, and miR-103a-3p served as a constitutive control. The data in the graphs represent the mean ± SEM. (C) Stable miR-28-3p and miR-193a-5p overexpression in RH30 cells promoted the percentage of cells in G0/G1 phase and inhibited the percentage of cells in S phase (representative results). (D) Transient miR-28-3p and miR-193a-5p overexpression in RH41 cells promoted the percentage of cells in G0/G1 phase and inhibited the percentage of cells in S phase (representative results). (E) Transient miR-28-3p and miR-193a-5p overexpression in RD cells inhibited the percentage of cells in S phase (representative results). *p < 0.05, **p < 0.01, ***p < 0.001.

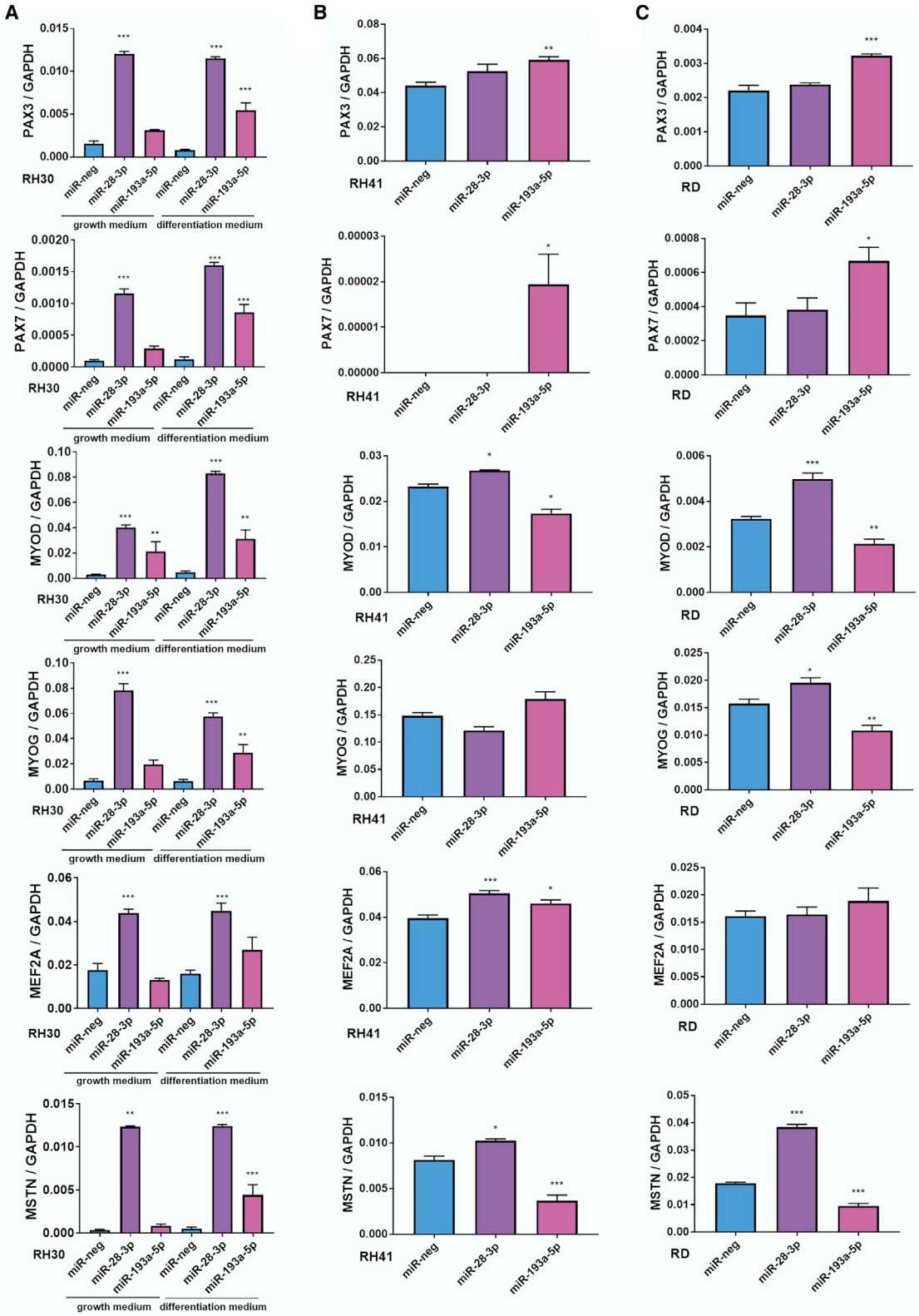

(legend on next page)

and slightly affected the morphology of RD cells (Figure S5A). Their overexpression also inhibited the proliferation of RH30, RH41, and RD cells, evaluated by cell counting (Figure S5B). miR-28-3p and miR-193a-5p inhibited the proliferation of RH30 cells, as higher percentages of cells were in G0/G1 phase, whereas lower percentages were in S phase (Figure 1C). Similar effects on the cell cycle were detected in transiently transfected RH41 (Figure 1D) and RD cells; however, in RD cells, miR-28-3p was the most efficient (Figure 1E).

miR-28-3p and miR-193a-5p are crucial regulators of the myogenic differentiation of RMS cells and myoblasts

Spindle-shaped cells and the inhibition of proliferation suggested that these miRNAs may be novel, important regulators of the myogenic differentiation of RMS cells. To further investigate this phenomenon, we evaluated expression levels of myogenic-related factors (early myogenic-related factors: PAX3 - paired box 3 and PAX7 - paired box 7; late myogenic regulatory factors: MYOD - myogenic differentiation 1 and MYOG - myogenin; and potentiator of myogenic factors: MEF2A - myocyte enhancer factor 2A and myokine: MSTN - myostatin) in three RMS cell lines: RH30 (Figure 2A), RH41 (Figure 2B), and RD (Figure 2C). Both miR-28-3p and miR-193a-5p were important regulators of myogenic-related factors but had slightly different effects on different cell lines, which probably depended on the different myogenic status of each cell line (Figure 2). In RH30 ARMS cells, miR-28-3p exerted stronger effects than miR-193a-5p in cells cultured in both DMEM with 10% fetal bovine serum (FBS) (growth medium) and DMEM with 2% horse serum (HS) (differentiation medium). miR-28-3p upregulated both early and late factors, such as PAX3, PAX7, MYOD, MYOG, MEF2A, and MSTN, whereas miR-193a-5p upregulated PAX3, PAX7, MYOD, MYOG, and MSTN, with stronger effects on differentiating cells (Figure 2A). In RH41 ARMS cells, miR-28-3p upregulated MYOD, MYOG, MEF2A, and MSTN, whereas miR-193a-5p upregulated the early factors PAX3 and PAX7, as well as MEF2A, and downregulated MYOD and MSTN (Figure 2B). In RD ERMS cells, miR-28-3p upregulated the late factors MYOD and MYOG, as well as MSTN, whereas miR-193a-5p upregulated the early factors PAX3 and PAX7 and downregulated the late factors MYOD and MYOG, as well as MSTN (Figure 2C). We also validated the expression of myosin heavy chain 2 (MYH2), the isoform that is expressed in fast-type skeletal muscle fibers.[27] MYH2 mRNA was expressed at very low levels in RH30 and RH41 cells and was not detected in RD cells. miR-28-3p slightly upregulated MYH2 levels in RH30 and RH41 cells (Figure S6A). Single RH30 cells overexpressing miR-28-3p and single RH41 cells overexpressing miR-28-3p and miR-193a-5p displayed fast myosin skeletal heavy chain (MyHC) protein expression (Figure S6B). Interestingly, the pattern of PAX3-FOXO1 expression levels in RH30 and RH41 ARMS cells was similar to the PAX3 expression levels, and in RH30 cells miR-28-3p was a strong inducer of PAX3-FOXO1 (Figure S6C). These results suggest that in the ERMS subtype, miR-28-3p induces late factors important in myogenic differentiation, whereas miR-193a-5p may be an inducer of early factors. Interestingly, in the ARMS subtype, miR-28-3p and miR-193a-5p may also be important regulators of both early and late factors crucial in myogenic differentiation.

To verify the effects of the candidate miRNAs on myogenic differentiation under not only pathologic but also normal conditions, we transfected human myoblasts with miRNA mimics, which led to the overexpression of miR-28-3p and miR-193a-5p, but the levels of the second strands were not upregulated (Figure 3A). Interestingly, miR-193a-5p tended to upregulate a known myogenic-related miRNA, miR-206 (Figure 3A), similar to the effect observed previously in RMS cells (Figure S4E). Twenty-four hours after transfection, myoblasts were differentiated for the next 48 h in medium with 2% HS, and subsequently the expression levels of myogenic-related factors were evaluated (Figure 3B). miR-28-3p upregulated the levels of the late factors MYOD and MYOG, as well as MYH2, MEF2A, and MSTN, whereas miR-193a-5p upregulated the levels of both the early and late factors PAX3, PAX7, MYF5, MYOD, and MYOG, as well as MEF2A, but downregulated the levels of MSTN (Figure 3B). Indeed, both miR-28-3p and miR-193a-5p increased cell fusion and the appearance of multinucleated myotubes with MyHC protein expression (Figure 3C). Interestingly, myoblasts overexpressing miR-193a-5p displayed an increased number of cells with high levels of the MyHC protein (Figure 3C) despite decreased MYH2 mRNA expression (Figure 3B). These results suggest that both miRNAs are crucial regulators of normal and pathologic myogenic differentiation.

miR-28-3p and miR-193a-5p inhibit the motility, chemotaxis, invasion, and adhesion of RMS cells and exhibit proangiogenic effects

Since not only proliferation and differentiation but also metastatic and proangiogenic capabilities are responsible for tumor growth, in the next step we evaluated the effects of the candidate miRNAs on the motility of RMS cells. miR-28-3p and miR-193a-5p inhibited the motility of RH30, RH41, and RD cells in the scratch assay (Figure 4A). Furthermore, they inhibited chemotaxis of those three cell lines toward hepatocyte growth factor (HGF) and stromal cell-derived factor 1 (SDF-1) (Figure 4B). Accordingly, invasion through Matrigel toward HGF and SDF-1 was inhibited in RH30 cells overexpressing miR-28-3p and miR-193a-5p (Figure 4C). Moreover, the adhesion of RH30 cells treated with HGF and SDF-1 to human umbilical vein endothelial cells (HUVECs) treated with tumor necrosis factor (TNF)-α was diminished (Figure 4D). These results suggested

Figure 2. miR-28-3p and miR-193a-5p regulated the expression levels of myogenic-related factors in RMS cells

(A–C) PAX3, PAX7, MYOD, MYOG, MEF2A, and MSTN mRNA levels were evaluated in RH30 cells (A) (n = 4) cultured in DMEM with 10% FBS (undifferentiated cells; growth medium) and DMEM with 2% HS (differentiated cells; differentiation medium) and in RH41 undifferentiated cells (B) (n = 3–4) and RD undifferentiated cells (C) (n = 3–4). qPCR results were calculated with the ΔCt method, and GAPDH served as a constitutive control. The data in the graphs represent the mean ± SEM. *$p < 0.05$, **$p < 0.01$, ***$p < 0.001$.

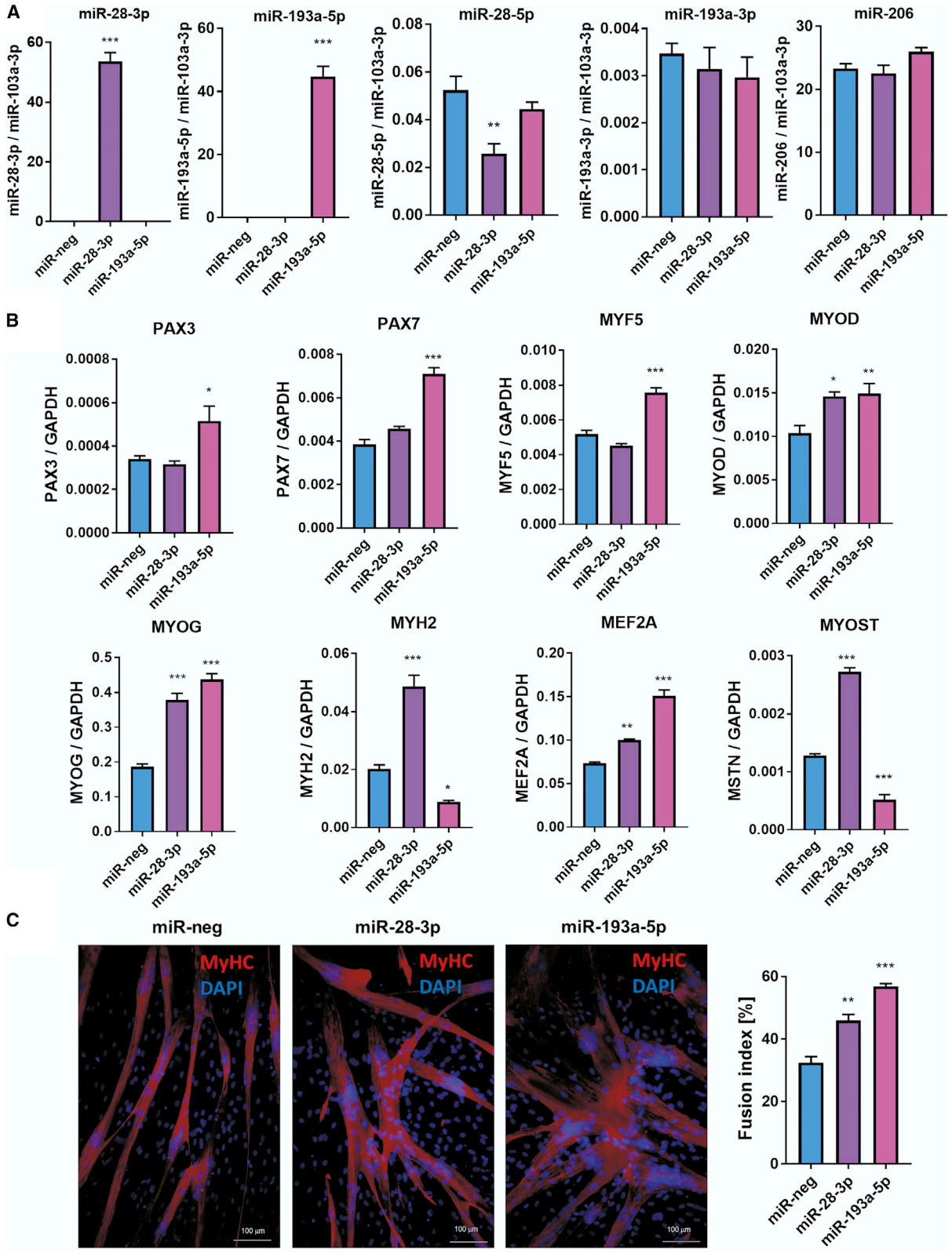

(legend on next page)

that the prometastatic capabilities of RMS cells were diminished *in vitro*. Accordingly, we evaluated the expression levels of SDF-1 and HGF receptors CXCR4 and MET on the surface of RH30 RMS cells by flow cytometry. CXCR4 was diminished in cells overexpressing miR-28-3p (24.96%) and miR-193a-5p (25.74%) compared with control cells (41.58%) (Figure S7A), whereas MET receptor levels were not significantly regulated by either miR-28-3p (59.55%) or miR-193a-5p (52.74%) compared with control cells (56.54%) (Figure S7B).

Surprisingly, miR-28-3p and miR-193a-5p increased the proangiogenic effects induced by RMS cells. Conditioned media from miR-28-3p- and miR-193a-5p overexpressing RH30 cells increased the number of tubule-like structures formed by HUVECs in the Matrigel assay (Figure 5A). The numbers of junctions (Figure 5B), master junctions (Figure 5C), and nodes (Figure 5D) were increased. These proangiogenic effects may be explained by the enhanced vascular endothelial growth factor (VEGF) protein levels in the medium from RH30 cells overexpressing miR-28-3p and miR-193a-5p (Figure 5E). Similarly, VEGF mRNA levels were increased in RD cells overexpressing miR-28-3p and miR-193a-5p (Figure 5F) and in RH41 cells overexpressing miR-28-3p (Figure 5G).

miR-28-3p and miR-193a-5p regulate RMS tumor growth, morphology, vascularization, and engraftment *in vivo*

To evaluate the effects of the candidate miRNAs not only *in vitro* but also *in vivo*, RH30 cells stably overexpressing miR-28-3p and miR-193a-5p were subcutaneously implanted into immunodeficient NOD-SCID mice (Figure 6). Subcutaneous xenotransplantation of RH30 cells led to the formation of tumors overexpressing miR-28-3p and miR-193a-5p (Figure 6A), with fibrotic structures displaying a diminished proliferation rate (Ki67 level) and, surprisingly, large, abnormal blood vessels, visualized with staining against CD31 (Figure 6B; Figure S8). Nevertheless, miR-28-3p and miR-193a-5p did not affect tumor size (Figure 6C) or weight (Figure 6D) at the end of the experiment. miR-28-3p overexpression increased PAX3, MYOD, MSTN, and VEGF levels in the tumors and tended to increase MYOG levels, whereas miR-193a-5p increased MSTN and VEGF and tended to increase PAX3 and MYOG levels (Figure 6E).

The simultaneous overexpression of both miRNAs after transfection with miRNA mimics (Figures S9A and S9B) induced morphological changes (Figure 7A) and diminished tumor size (Figure 7B) and weight (Figure 7C), suggesting that the simultaneous expression of both miRNAs may give cumulative effects on RMS tumor growth. The effects on fibrotic structures, Ki67-positive cells, and CD31-positive capillaries resembled the previous results (Figure 7A; Figure S9C) The levels of factors regulating myogenic differentiation (PAX3, MYOD, MYOG, MEF2A, MSTN, MYH2) were also increased in tumors simultaneously overexpressing both miR-28-3p and miR-193a-5p (Figure 7D). Interestingly, intravenous injection of RH30 cells simultaneously overexpressing both miR-28-3p and miR-193a-5p resulted in diminished engraftment of the cells in murine organs 24 h after injection (Figure 7E) and inhibited engraftment into murine bone marrow 7 days after injection (Figure 7F). These results may be the effect of diminished cell migration, adhesion, and proliferation. Furthermore, they suggest that simultaneous miR-28-3p and miR-193a-5p regulation is crucial in tumor growth and metastasis, similar to SNAIL action.

DISCUSSION

This study was undertaken to investigate the role of SNAIL-dependent miRNAs in the regulation of RMS growth and metastasis, since the SNAIL-miRNA pathway has been demonstrated previously to be a crucial regulator of RMS differentiation and migration.[11] The SNAIL transcription factor is a crucial regulator of RMS growth and differentiation, and SNAIL-deficient RMS cells do not form any tumors in immunodeficient mice.[6] Current literature suggests that SNAIL is a crucial regulator of miRNAs by binding directly to their promoters or regulatory elements or by indirect action via mediators.[7] Therefore, based on previous miRNA sequencing results,[11] we selected two candidate miRNAs that were the most potently regulated by the SNAIL transcription factor for further research. In our current studies, we sought to identify the precise roles of miR-28-3p and miR-193a-5p in RMS that may also be important in other tumor types or myogenic differentiation.

SNAIL-deficient RMS cells displayed enhanced expression of miR-28-3p and miR-193a-5p, but they seemed to be rather indirectly regulated by SNAIL, since ChIP-seq analysis did not reveal significant SNAIL binding to their promoters or regulatory regions. Nevertheless, ChIP-seq analysis revealed that SNAIL bound to promoters of miR-3191 and miR-8072 and to the intron of the MIR193BHG gene, which harbors regulatory enhancer features active in certain cell types, according to the Ensembl database (human GRCh38.p13).[26] Since the expression of those miRNAs was not detected in RMS cells via miRNA sequencing, this finding may be of greater significance for other tumor types.

The origin of RMS tumors is associated with an impaired myogenic differentiation, and forcing RMS tumors to differentiate may be a novel

Figure 3. miR-28-3p and miR-193a-5p regulated the differentiation of myoblasts

(A) miR-28 3p and miR-193a-5p were temporally overexpressed in myoblasts after transfection with miRNA mimics, which did not affect the levels of the second strands; 24 h after transfection, myoblasts were treated with a differentiating medium containing 2% HS for the next 48 h and the miRNA overexpression level was validated with qPCR; n = 4. (B) miR-28-3p and miR-193a overexpression regulated myogenic-related factors in differentiating myoblasts, n = 4. (C) miR-28-3p and miR-193a overexpression increased the number of myotubes with high MyHC expression and induced their fusion. The photos are representative merged images of immunofluorescent staining for MyHC (MyHC: red; nuclei: Hoechst, blue) in myotubes. The fusion index was calculated by expressing the number of nuclei within MyHC-positive myotubes with ≥2 nuclei as a percentage of the total nuclei (n = 3). The white scale bars represent 100 μm. qPCR results were calculated with the ΔCt method, and miR-103a-3p or GAPDH served as a constitutive control. The data in the graphs represent the mean ± SEM. *p < 0.05, **p < 0.01, ***p < 0.001.

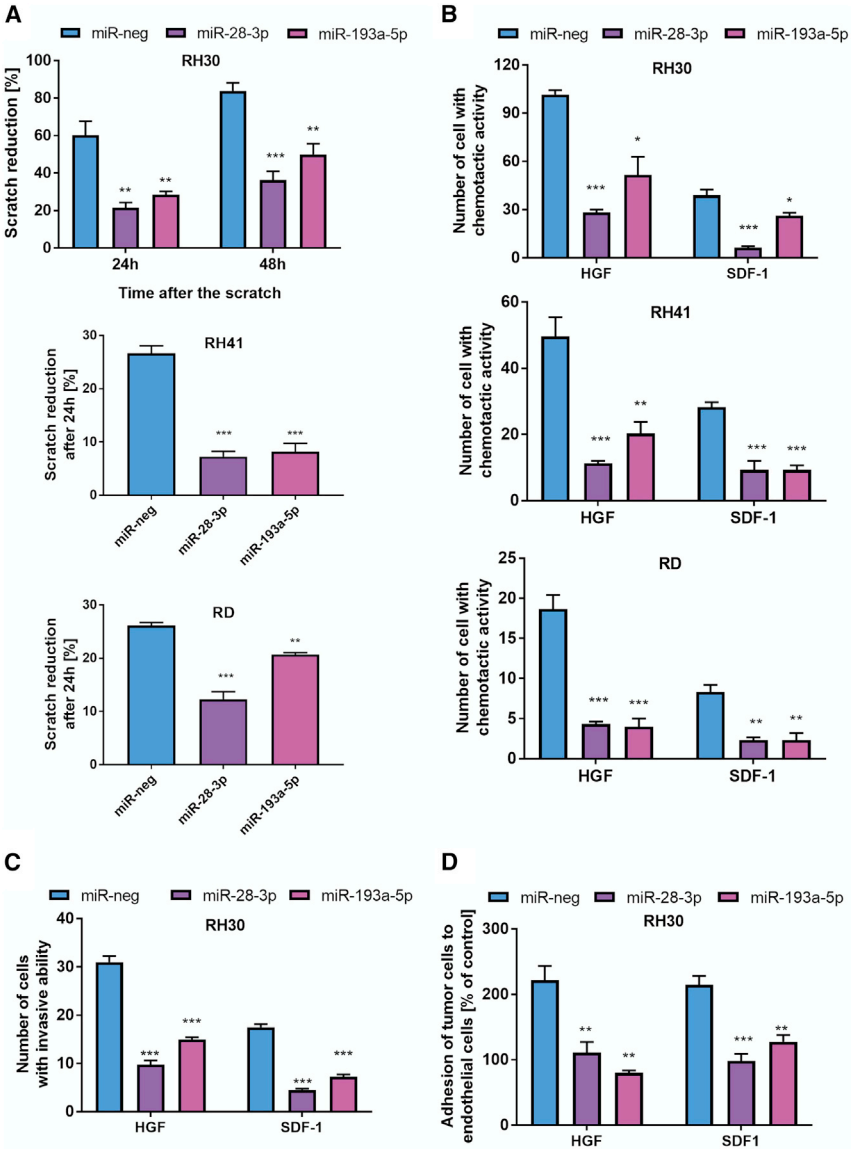

Figure 4. miR-28-3p and miR-193a-5p inhibited the motility, chemotaxis, invasion, and adhesion of RMS cells

(A) miR-28-3p and miR-193a-5p overexpression in RH30, RH41, and RD cells inhibited migration, as determined via the scratch assay; n = 3. (B) miR-28-3p and miR-193a-5p overexpression in RH30, RH41, and RD cells inhibited chemotaxis toward HGF and SDF-1; n = 3. (C) miR-28-3p and miR-193a-5p overexpression in RH30 cells inhibited invasion through Matrigel toward HGF and SDF-1; n = 3. (D) miR-28-3p and miR-193a-5p overexpression in RH30 cells inhibited adhesion of tumor cells treated with HGF and SDF-1 to HUVECs treated with TNF-α; n = 3. The data in the graphs represent the mean ± SEM. *p < 0.05, **p < 0.01, ***p < 0.001.

therapeutic tool.[1] RMS cells do not complete normal myogenic differentiation despite the expression of several myogenic factors.[2] One of the novel crucial factors that regulates the myogenic differentiation of RMS tumors is the SNAIL transcription factor, which may regulate the level and activity of myogenic factors directly or indirectly.[6] One of the indirect mediators of SNAIL action on myogenic differentiation may be miRNAs, such as miR-28-3p or miR-193a-5p. Previous studies identified them to be upregulated in differentiating myoblasts[25] and in SNAIL-deficient RMS cells,[11] which suggested their potential roles in myogenic differentiation. Nevertheless, our current studies for the first time identified them as novel myogenic-related miRNAs that regulate normal differentiation of myoblasts or the pathologic differentiation of RMS cells because of their action as inducers of myogenic factors in both cell types. Importantly, both miR-28-3p and miR-193a-5p inhibited the proliferation of RMS cells, arrested the cells in G0/G1 phase, and simultaneously induced the expression of myogenic-related factors. The successful switch from proliferation to differentiation is a key event in differentiating myoblasts and RMS tumors.[2] Similar effects were observed in SNAIL-deficient RMS cells,[6] confirming that these miRNAs may be important mediators of SNAIL action. Nevertheless, miR-28-3p and miR-193a-5p differentially regulated the expression levels of myogenic-related factors, and this regulation seemed to be dependent on the myogenic status of the cells. Myogenesis is regulated by different early and late myogenesis-related factors, and their expression levels were analyzed in our current study. PAX3 and PAX7 are master regulators of early lineage specification, whereas MYF5 and MYOD are responsible for the commitment of cells to the myogenic program. Subsequently, the expression of both MYOG and MRF4 is required for the fusion of myocytes and the formation of myotubes with high MyHC levels.[28] Based on these observations, our current results suggest that miR-28-3p in myoblasts and ERMS may be an inducer of late factors important in differentiation steps, whereas in ARMS it may induce both early and late factors. miR-193a-5p induces both early and late factors important in the differentiation of myoblasts and ARMS, whereas, surprisingly, in ERMS it may be an inducer of early factors and an inhibitor of late factors. Surprisingly, to significantly inhibit RMS tumor growth *in vivo*, the simultaneous expression of both miR-28-3p and miR-193a-5p is required, probably because of their cumulative effects on myogenic differentiation. This agrees with our results showing that SNAIL inhibits RMS growth,[6] since both miR-28-3p and miR-193a-miRNA are regulated by SNAIL.[11] miR-28-3p and miR-193a-5p may join the list of miRNAs that can inhibit RMS growth by promoting myogenic differentiation. Such effects have been described previously for miR-206,[21] miR-450b-5p,[22] miR-29,[23] and miR-411-5p.[24] The inhibitory effects of miR-193a-5p on tumor growth or the proliferation and survival of

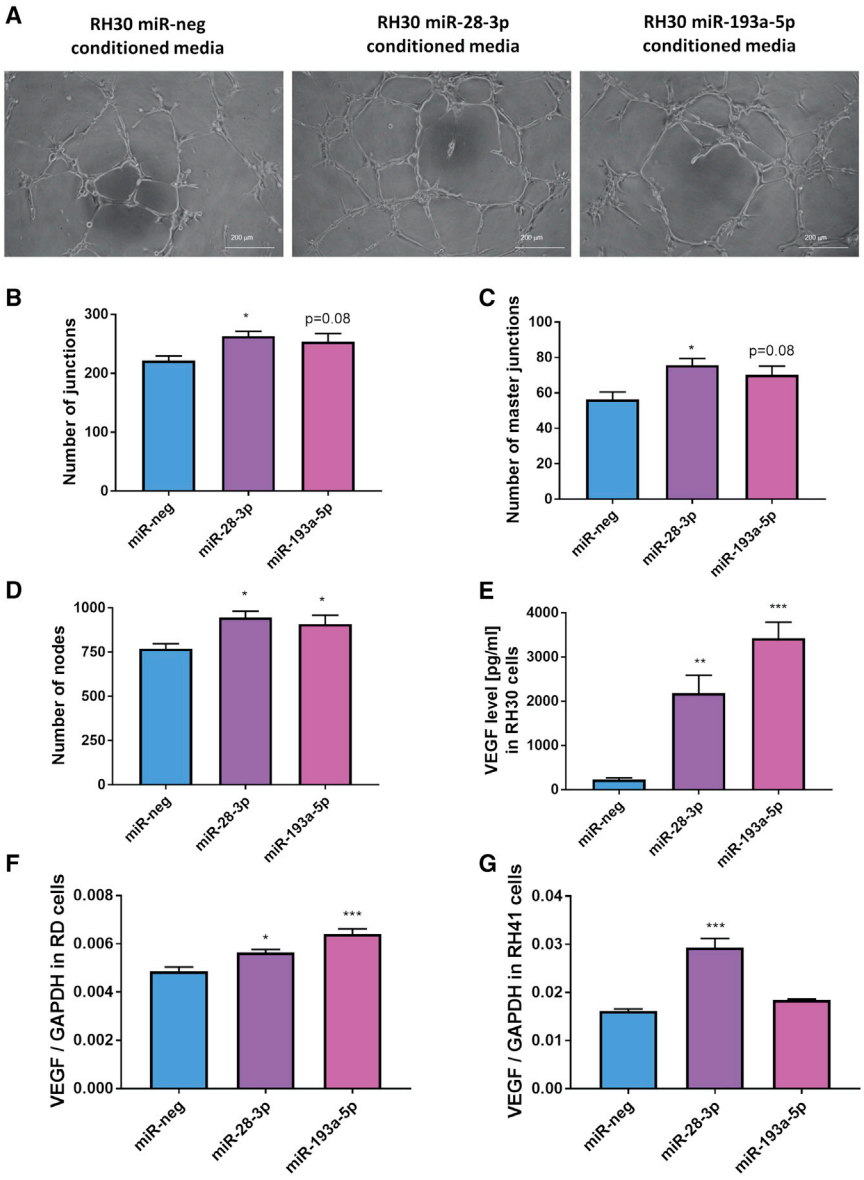

Figure 5. miR-28-3p and miR-193a-5p induced proangiogenic effects *in vitro* in RMS cells by upregulating VEGF

(A–D) Conditioned media from RH30 cells overexpressing miR-28-3p and miR-193a-5p increased the number of tubule-like structures formed by HUVECs in the Matrigel angiogenesis assay *in vitro* (A) (representative images) and slightly increased the numbers of junctions (B), master junctions (C), and nodes (D); n = 5. (E–G) miR-28-3p and miR-193a-5p overexpression increased VEGF protein levels secreted into the culture medium in RH30 cells (E) (ELISA, n = 3) and slightly upregulated VEGF mRNA levels in RD cells (F) (n = 4), whereas in RH41 cells (G) (n = 3), only miR-28-3p upregulated VEGF mRNA levels. qPCR results were calculated with the ΔCt method, and GAPDH served as a constitutive control. White scale bars represent 100 μm. The data in the graphs represent the mean ± SEM. *p < 0.05, **p < 0.01, ***p < 0.001.

regulate the migratory and metastatic capabilities of human colon cancer[13] and endometrial cancer[14] cells. The possible direct target of miR-193a-5p, which is suggested in the literature as an important mediator, again involves YY1 transcription factor.[14] This target was also predicted with miRDB[33] and TargetScanHuman 7.1[34] miRNA prediction tools.

Similar to miR-193a-5p, miR-28-3p also exerts effects on tumor proliferation and survival. It inhibits the growth of non-Hodgkin lymphoma[35] but, surprisingly, promotes colorectal carcinoma,[17] which suggests that it may play a different role in different tumor types. It may also regulate the survival of cardiomyocytes.[36] Based on previous data, miR-28-3p might exert these effects via the regulation of phosphatidylinositol signaling[18] or PDK1 (phosphoinositide-dependent kinase-1) /AKT kinase / mTOR (mechanistic target of rapamycin) signaling.[36]

tumor cells have been described previously in different tumor types, such as breast cancer,[29] endometrial adenocarcinoma,[14] and squamous cell carcinoma.[30] The literature suggests several possible direct targets of miR-193a-5p, but the most important one that may be responsible for regulation of both proliferation and myogenic differentiation of RMS cells is the YY1 (Yin Yang 1) transcription factor,[14] as its roles in skeletal myogenesis and RMS growth have been described previously.[23] Furthermore, YY1 was found to be associated with multiple myofibrillar promoters in myoblasts, such as MyHCIIb.[31] YY1 was also demonstrated to be important in RMS development as miR-29 target.[23] miR-193a-5p and its second strand miR-193a-3p were shown to be downregulated in lung cancer metastasis[32] and in metastatic osteosarcoma cells.[15] Furthermore, miR-193a-5p was demonstrated to

We demonstrated that in RMS cells miR-28-3p and miR-193a-5p diminish not only cell proliferation but also cell migration, chemotaxis, adhesion, and invasion. This agrees with our previous results showing the role of SNAIL in RMS metastasis,[11] since both miR-28-3p and miR-193a-5p are regulated by SNAIL.[11] We also previously demonstrated that miR-28-3p may regulate EZRIN expression and that the mechanism may explain differences in cell motility.[11] Similar effects were observed in other tumor types. miR-28-3p regulates the migration of colorectal cancer cells[17] and nasopharyngeal cancer cells.[37] It has prognostic significance in biochemical recurrence-free survival in patients with prostate cancer bone metastasis.[38] Nevertheless, previous investigations, such as in prostate cancer,[39] were more focused on miR-28-5p and not on miR-28-3p. The host gene for miR-28 is LPP (LIM

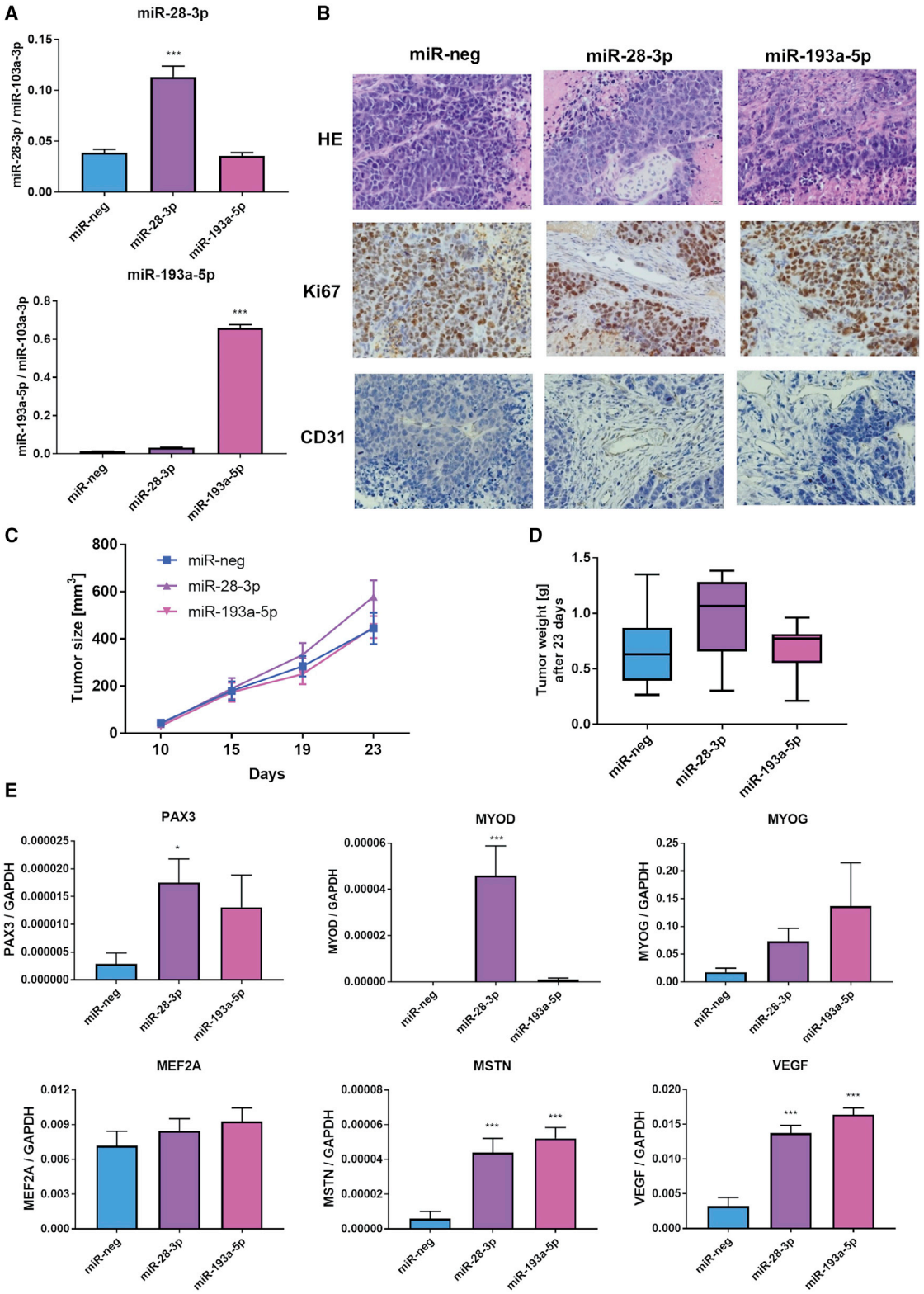

(legend on next page)

domain lipoma preferred partner),[16] a protein that localizes to the cell periphery in focal adhesions and may be involved in the adhesion, motility, and formation of invadopodia.[40]

Our studies also demonstrated the proangiogenic capabilities of miR-28-3p and miR-193a-5p in RMS cells, which resulted in abnormal tumor vasculature, probably due to an increased VEGF level. Pathologic angiogenesis is a common feature of tumor cells.[41] Furthermore, immune cells may infiltrate via blood vessels and attack tumor cells.[41] Despite the fact that these miRNAs probably induce pathologic angiogenesis with abnormal blood vessels, they downregulate the adhesion of RMS cells to endothelial cells. Therefore, RMS tumors may have difficulties spreading away and forming metastases despite enhanced vascularization. It cannot also be excluded that the generated blood vessels may not be fully functional. The proangiogenic properties of miR-193a-5p have been described in diabetic cardiomyopathy, possibly through the inverse regulation of its downstream insulin growth factor 2 (IGF2) gene.[42] Furthermore, miR-28 is a member of a group of 16 miRNAs that may serve as promising prognostic markers in primary central nervous system lymphoma and may regulate angiogenesis and cell migration.[43]

miR-28-3p and miR-193a-5p also induced formation of fibrotic structures in RMS tumors growing in mice. Similar fibrotic structures were observed in RMS tumors treated with small interfering RNA (siRNA) against SNAIL,[6] which suggests that miR-28-3p and miR-193a-5p might be important mediators of SNAIL action. miR-193a-5p was previously associated with myocardial fibrosis in patients with hypertrophic cardiomyopathy[44] and liver fibrosis,[45] whereas miR-28-3p was associated with glomerular capillaries during antibody-mediated rejection.[46]

To conclude, we identified miR-28-3p and miR-193a-5p as miRNAs that are significantly regulated by the SNAIL transcription factor in RMS. They were demonstrated to be important mediators of SNAIL action. Both miR-28-3p and miR-193a-5p are novel myogenic-related miRNAs involved in both normal and pathologic myogenic differentiation as inducers of myogenic factors. Nevertheless, only the simultaneous expression of both can inhibit RMS tumor growth *in vivo*. miR-28-3p and miR-193a-5p also diminish RMS progression by regulating cell migration, chemotaxis, invasion, and adhesion, as well as vascularization. Understanding the molecular mechanisms of miRNA actions may help develop novel therapeutic strategies that may be based on miRNA mimics. Previously, therapeutic molecules based on miRNA sequences were established, and some have shown promising results in human clinical trials.[47]

MATERIALS AND METHODS

Cell culture

RMS cell lines (RH30, RH41, and RD) were kindly provided by Dr. P.J. Houghton (Center for Childhood Cancer, Columbus, OH, USA). The cells were cultured in high-glucose DMEM medium (Lonza Group Ltd., Basel, Switzerland) supplemented with 10% FBS (EURx, Gdansk, Poland) and 50 μg/mL gentamicin (Lonza) at 37°C, under 5% CO_2 and with 95% humidity. The cell lines were routinely tested for *Mycoplasma spp.* contamination with the MycoAlert Mycoplasma Detection Kit (Lonza). RMS cell line authentication was performed by short tandem repeat (STR) profiling using an AmpFlSTR SGM PLUS Kit (Applied Biosystems, Foster City, CA, USA) and an ABI Prism 310 Genetic Analyzer (Applied Biosystems) according to the manufacturer's protocol.

The RMS cell lines were differentiated in low-glucose DMEM medium (Lonza) supplemented with 2% HS (Gibco BRL, Grand Island, NY, USA). The cellular morphology was visualized with Wright's stain (Sigma-Aldrich, St. Louis, MO, USA).

Primary human myoblasts were isolated by our laboratory and characterized previously.[48] These cells were cultured in DMEM/F12 medium (Lonza) supplemented with dexamethasone and insulin (both from Sigma-Aldrich), 18% FBS (EURx), epidermal growth factor (EGF; R&D Systems, Minneapolis, MN, USA), FGF (R&D), HGF (R&D), and gentamicin (Lonza). They were differentiated in low-glucose DMEM medium (Lonza) supplemented with 2% HS (Gibco).

HUVECs were ordered from Becton Dickinson Biosciences and cultured in endothelial cell growth medium (PromoCell, Heidelberg, Germany) with endothelial cell growth supplement (PromoCell).

Transduction of cells with viral vectors

RH30 cells were transduced with shRNA lentiviral particles targeting SNAIL and control lentiviral particles (Santa Cruz Biotechnology, Santa Cruz, CA, USA) and characterized as described previously.[6] Viral vectors encoding luciferase were generated as described previously[49] with a plasmid encoding luciferase (Addgene, Watertown, MA, USA). Subsequently, RH30 cells were transduced with those vectors with a protocol described previously.[49]

Transfection of cells with miRNA precursors and inhibitors

RH41, RD, and RH30 cells were transfected with 30 nM mirVana miRNA mimics hsa-miR-28-3p (ID: MC12933), hsa-miR-193a-5p

Figure 6. miR-28-3p and miR-193a-5p regulated RMS tumor morphology, myogenic differentiation, and vascularization *in vivo*

(A) RH30 cells overexpressing miR-28-3p and miR-193a-5p were subcutaneously implanted into immunodeficient NOD-SCID mice, and miRNA expressions levels were evaluated in the growing tumors; n = 10. (B) miR-28-3p and miR-193a-5p overexpression in RH30 cells induced fibrosis (hematoxylin and eosin [HE] staining) and inhibited proliferation (Ki67 staining) but induced the formation of large abnormal tumor vessels (CD31 staining) 23 days after the subcutaneous implantation of 5×10^6 RH30 cells into immunodeficient NOD-SCID mice; representative images of immunohistochemical staining are shown. (C and D) miR-28-3p or miR-193a-5p overexpression in RH30 subcutaneous xenotransplants did regulate tumor size (C) measured with caliper and tumor weight (D) (whisker plot, min to max) at the end of the experiment; n = 10. (E) PAX3, MYOD, MYOG, MEF2A, MSTN, and VEGF mRNA levels were evaluated in tumors (n = 5). qPCR results were calculated with the ΔCt method, and GAPDH served as a constitutive control. The data in the graphs represent the mean ± SEM. White scale bars represent 20 μm. *p < 0.05, **p < 0.01, ***p < 0.001.

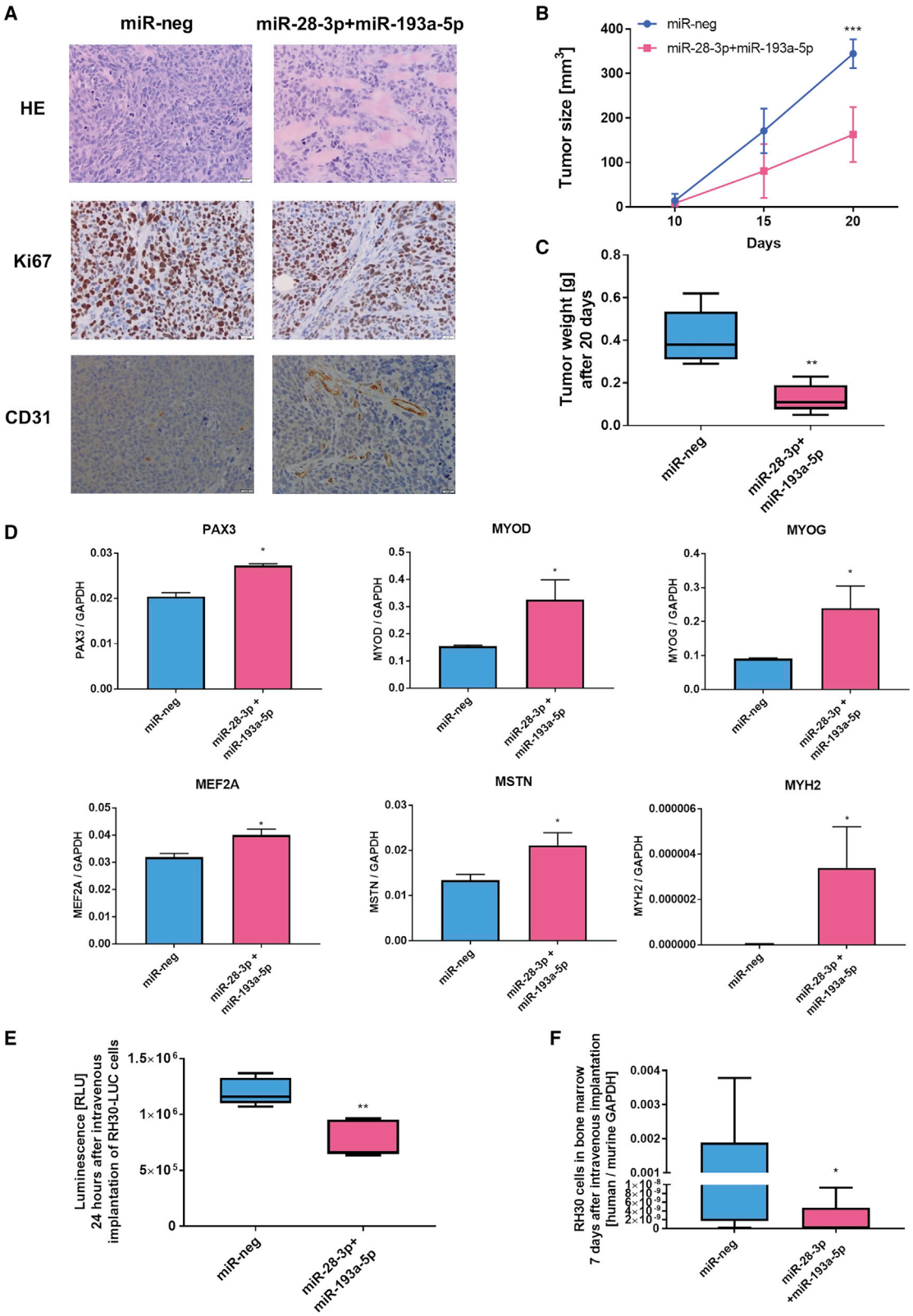

(legend on next page)

(ID: MC1178), and negative control 1 using Lipofectamine RNAiMAX (Invitrogen) transfection reagent according to the vendor's protocol. RNA was isolated 72 h after transfection or the cells were seeded for further experiments 24–48 h after transfection.

Transduction of cells with lentiviral vectors encoding miRNAs

RH30 cells were transduced with MISSION Lenti miRNA particles (Sigma-Aldrich) encoding hsa-miR-28-3p (HLMIR0426), hsa-miR-193a-5p (HLMIR0313), or human negative control 1 (cat. no. NCLMIR001) at an MOI of 5 according to the vendor's protocol. Transduced cells were selected with 0.5 μg/mL puromycin (InvivoGen, San Diego, CA, USA).

Cell cycle and BrdU assays

For the assessment of DNA content and bromodeoxyuridine (BrdU) incorporation, RH30 cells stably overexpressing miRNAs were starved in DMEM medium with 0.5% bovine serum albumin (BSA) for 2 days and then treated with 10% FBS for 1 day. RH41 and RD cells were transfected and seeded for the experiment 24 h after transfection. They were starved in DMEM medium with 0.5% BSA for 1 day and then treated with 10% FBS for 1 day. Subsequently, the cells were analyzed with an APC BrdU Flow Kit (BD Pharmingen, California, USA) using an Attune flow cytometer (Thermo Fisher Scientific), according to the vendor's protocol.

RNA isolation and reverse transcription

Total RNA was extracted with a GeneMATRIX Universal RNA/miRNA Purification Kit (EURx) or a mirVana miRNA Isolation Kit (Ambion) according to the manufacturer's protocol. Reverse transcription of mRNA was performed with Moloney Murine Leukemia Virus (MMLV) reverse transcriptase (Promega, Madison, WI, USA) according to the vendor's protocol. Reverse transcription of miRNA was performed with a Universal cDNA Synthesis Kit (Exiqon, Denmark) or a miRCURY LNA RT Kit (QIAGEN) according to the manufacturers' protocols.

Quantitative real-time PCR

Gene expression was determined by quantitative real-time PCR analysis using the QuantStudio 7 Flex Real-Time PCR System (Applied Biosystems, Foster City, CA, USA), Blank qPCR Master Mix (EURx), and the indicated TaqMan probes (Applied Biosystems): human: GAPDH (Hs99999905_m1), MYF5 (Hs00271574_m1), MYOD (Hs00159528_m1), MRF4 (Hs01547104_g1), MEF2A (Hs01050409_m1), MYOSTATIN/MSTN (Hs00976237_m1), MYOGENIN (Hs01032275_m1), MyHC (Hs00430042_m1), PAX3 (Hs00240950_m1), PAX7 (Hs00242962_m1), and VEGF (Hs00173626_m1). The mRNA expression levels of all of the samples were normalized to the housekeeping gene GAPDH by the $2^{-\Delta Ct}$ method.

PAX3-FOXO1 levels were evaluated with SYBR Green qPCR Master Mix (EURx) and the following primers:

PAX3-FOXO1 forward: 5′-AACCCCACCATTGGCAATG-3′

PAX3-FOXO1 reverse: 5′-ACCCTCTGGATTGAGCATCCA-3′

Its level was normalized to that of the housekeeping gene GAPDH with the $2^{-\Delta Ct}$ method.

For the evaluation of miRNA expression by quantitative real-time PCR, SYBR Green qPCR Master Mix (EURx) with an LNA PCR primer set (Exiqon) or the miRCURY LNA miRNA PCR Assay (QIAGEN) for human miR-28-3p, miR-193a-5p, miR-28-5p, miR-193a-3p, miR-206, and miR-103a-3p was used. miRNA expression levels were quantified with the $2^{-\Delta Ct}$ method, and miR-103a-3p served as a relative control (selected based on previous sequencing results).[11]

MicroRNA sequencing data

miRNA NGS data described in the current manuscript were deposited previously into the GEO database under accession number GSE100114, and the analysis was described previously.[11]

Western blot analysis

Total protein extracts were isolated with M-PER lysis buffer (Pierce, Rockford, IL, USA) as described previously[5] according to the manufacturer's protocol. The protein concentration was measured with the Bradford protein assay (Bio-Rad, Hercules, CA, USA) according to the vendor's protocol. Western blotting was performed with the anti-GAPDH rabbit monoclonal antibody (mAb) (14C10; #2118; Cell Signaling Technology, Leiden, the Netherlands), the anti-SNAIL mouse mAb (L70G2; #3895; Cell Signaling), and secondary anti-rabbit and anti-mouse antibodies conjugated with horseradish peroxidase (HRP, Santa Cruz Biotechnology). Proteins were separated by electrophoresis on a 12% resolving sodium dodecyl sulfate-PAGE gel, and the fractionated proteins were transferred to a polyvinylidene fluoride (PVDF) membrane (Bio-Rad). Chemiluminescent signals were

Figure 7. Simultaneous overexpression of both miR-28-3p and miR-193a-5p regulated tumor growth, morphology, vascularization, myogenic differentiation, and engraftment *in vivo*

(A) Simultaneous overexpression of both miR-28-3p and miR-193a-5p by transfection with miRNA mimics induced fibrosis (hematoxylin and eosin staining) and inhibited proliferation (Ki67 staining) but induced formation of large abnormal tumor vessels (CD31 staining) 20 days after subcutaneous implantation of 1×10^6 RH30 cells in Matrigel into immunodeficient NOD-SCID mice. (B and C) Simultaneous overexpression of both miR-28-3p and miR-193a-5p by transfection with miRNA mimics diminished tumor size (B) (estimated with calipers) and tumor weight (C) 20 days after the subcutaneous implantation of 1×10^6 RH30 cells in Matrigel into immunodeficient NOD-SCID mice; n = 5. (D) PAX3, MYOD, MYOG, MEF2A, MSTN, and MYH2 mRNA levels were evaluated in tumors (n = 5). qPCR results were calculated with the ΔCt method, and GAPDH served as a constitutive control. (E and F) Simultaneous overexpression of both miR-28-3p and miR-193a-5p by transfection with miRNA mimics diminished engraftment into murine organs 24 h after the intravenous injection of RH30 cells expressing luciferase into immunodeficient NOD-SCID mice (E) (evaluation of the luminescence level with imaging equipment) and inhibited engraftment into the bone marrow after 7 days (F) (evaluation of the human GAPDH to murine GAPDH mRNA ratio by qPCR); n = 5. White scale bars represent 20 μm. The data in the graphs represent the mean ± SEM. *$p < 0.05$, **$p < 0.01$, ***$p < 0.001$.

developed with SuperSignal West Pico PLUS Chemiluminescent Substrate (Thermo Scientific) and the ChemiDoc MP Imaging System (Bio-Rad). Densitometric analysis of western blot images was performed with ImageLab software (Bio-Rad). The ratio of the adjusted volume band of the gene of interest to the constitutive gene was evaluated, and subsequent results are presented as the percentage of the control.

ELISA

VEGF levels in media collected from the transduced cells were analyzed with a LEGEND MAX Human VEGF ELISA Kit on a pre-coated plate (BioLegend, San Diego, CA, USA), according to the vendor's protocol.

Bioinformatic analysis of miRNA targets

Bioinformatic analysis of miR-28-3p and miR-193a-5p targets was performed with miRDB (http://mirdb.org/)[33] and TargetScanHuman 7.1 (http://www.targetscan.org/vert_71/).[34] The online website tools were accessed on May 6th, 2020.

Chromatin immunoprecipitation data

ChIP-seq data described in the current manuscript were deposited previously into the GEO database under accession number GSE152355, and the analysis was described previously.[11] IGV[50] was used as a visualization tool for the interactive exploration of large, integrated genomic datasets from ChIP-seq results deposited in the GEO database under accession number GSE152355. Regulatory regions of the MIR28 and MIR193A genes were analyzed. Furthermore, regulatory enhancer features were screened in the Ensembl database (Human GRCh38.p13).[26]

Scratch assay

Confluent RH30, RH41, and RD cells were treated with DMEM with 0.5% BSA for 24 h. Subsequently, a scratch was generated with a pipette tip. Starving medium was replaced every day. Photographs were taken after 24 or 48 h and analyzed with ImageJ software (National Institutes of Health, Bethesda, MD, USA).

Chemotaxis assay

The chemotaxis of RH30, RH41, and RD cells to 20 ng/mL HGF (R&D Systems) and 100 ng/mL SDF-1 (PeproTech, Rocky Hill, NJ, USA) was evaluated with a modified Boyden's chamber with 8 μm pore polycarbonate membrane inserts (Transwell; Corning Life Sciences PZ HTL SA, Warsaw, Poland), as described previously.[5] BSA (0.5%) served as a negative control. Similarly, the invasion of RH30 cells through growth factor-reduced Matrigel invasion inserts (Corning Life Sciences) to 20 ng/mL HGF and 100 ng/mL SDF-1 was also investigated as described previously.[5]

Angiogenic Matrigel assay *in vitro*

RH30 cells were cultured on six-well plates for 24 h in DMEM with 2% FBS. Subsequently, the conditioned media were collected and mixed with medium for endothelial cells supplemented with 2% FBS at a ratio of 1:1. For the Matrigel assay, 50 μL of growth factor-reduced Matrigel (BD Biosciences) was plated into a 96-well plate and incubated at 37°C for 30 min. HUVECs were detached and counted, and single-cell suspensions at a density of 10,000 cells per well in 200 μL of conditioned media and proper controls were plated on the Matrigel. Subsequently, endothelial tube formation was photographed 6 h after seeding. The formation of tubule-like structures was analyzed with Angiogenesis Analyzer for ImageJ (available online: https://imagej.nih.gov/ij/macros/toolsets/Angiogenesis%20Analyzer.txt). The numbers of junctions, master junctions, and nodes were calculated.

Immunofluorescent staining

Myoblasts and RH30 and RH41 cells were fixed in 4% formaldehyde (POCH) in phosphate-buffered saline (PBS), permeabilized in 0.1% Triton X-100 (Sigma-Aldrich), blocked in 1% BSA (Sigma-Aldrich), incubated with the anti-fast myosin skeletal heavy chain antibody (MyHC, MY-32, ab51263, Abcam), and then incubated with secondary goat anti-mouse antibodies conjugated with Alexa Fluor 555 (Life Technologies) and Hoechst. To quantify myoblast fusion, we calculated the fusion index by expressing the number of nuclei within MyHC-positive cells with ≥ 2 nuclei as a percentage of the total nuclei. The stained slides were mounted with Dako Fluorescence Mounting Medium (Dako, Denmark). For morphology visualization, RH30, RD, and RH41 cells were stained with Wright's dye (Sigma-Aldrich).

Microscopy

Microscopic images were visualized with an Olympus IX70 or Olympus BX51 microscope (Olympus Corporation, Tokyo, Japan) and a Canon EOS1100D digital photo camera (Canon Inc., Tokyo, Japan) or an Olympus XC50 camera. The images were processed and analyzed with cellSens Dimension software or ImageJ software (National Institutes of Health, USA).

Flow cytometry

For the evaluation of MET and CXCR4 receptor expression levels, RH30 cells were stained with the monoclonal fluorescein isothiocyanate (FITC)-labeled anti-human HGFR/c-MET antibody, clone 95106 (R&D), phycoerythrin (PE)-labeled anti-human CXCR4 antibody (Becton Dickinson), or mouse IgG1 isotype control (R&D) labeled with FITC or PE. The cells were acquired and analyzed with an Attune Next Flow Cytometer and analyzed with Attune NxT Software v.2.2 (Thermo Fisher Scientific, USA).

Adhesion assay

HUVECs (5×10^4 per well) were seeded into black 96-well plates with a clear bottom (Corning Costar, Amsterdam, the Netherlands) and grown overnight to a confluent monolayer. After stimulation of endothelial cells with TNF-α (50 ng/mL) for 24 h, RMS cells were incubated with 2.5 μM calcein AM (BD Pharmingen) for 30 min at 37°C in cell culture medium, washed, allowed to rest for 30 min, and treated with 100 ng/mL SDF-1 for 15 min or 20 ng/mL HGF for 30 min, or they were in control medium without growth factors. 1×10^4 RH30 cells were added to the endothelial monolayers and

incubated at 37°C for 15 min. Plates were washed three times with PBS to remove unbound cells, and fluorescence was read with a fluorescence plate reader (Spark 10M multimode microplate reader, Tecan) at an excitation wavelength of 495 nm and an emission wavelength of 515 nm. The results were normalized to the percentage of the cells under control conditions.

In vivo experiments

Animal experiments were approved by the Local Ethics Committee in Krakow (no 12/2018 with modifications 208A/2018 and 212/2018).

RH30 cells (5×10^6) transduced with viral vectors encoding miRNAs in PBS were injected subcutaneously into 6- to 8-week-old NOD-SCID mice. Each experimental group comprised 10 animals. The experiments were repeated two times. Furthermore, 1×10^6 RH30 cells expressing luciferase and transfected with miRNA mimics in Matrigel with PBS (1:1) were injected subcutaneously into 6- to 8-week old NOD-SCID mice. The second model (with the transfected cells) involved a smaller number of cells because of the limited number of cells after transfection, and Matrigel was used to facilitate tumor growth from fewer cells in a short amount of time. In those models, tumor size was evaluated one or two times per week with a caliper, and tumor volume was estimated with the formula $V = D \times d^2 \times 0.5$ (V is tumor volume, D is the largest dimension, d is the smallest dimension). After ~3 weeks the mice were sacrificed, and their tumors and bone marrow cells were harvested. After tumor weight was determined, tumors were fixed in formalin. Tumor sections were stained with hematoxylin and eosin to visualize tumor morphology, and after deparaffinization they were stained immunohistochemically as described previously,[5] with the anti-Ki67 primary mouse monoclonal antibody to evaluate tumor proliferation (clone MIB-1; 1:75, DakoCytomation, Denmark, UK) and the anti-CD31 antibody to visualize tumor vascularization (1:50, Abcam, ab28364). The percentages of fibrotic structures, Ki67-positive cells, and CD31-positive capillaries were calculated with ImageJ software (National Institutes of Health, USA).

To study metastasis, we used an intravenous injection model, which is a broadly used model that attains migration through blood vessels and engraftment in niche locations but may omit the initial steps of metastasis.[51] In that model, 1×10^6 RH30 cells expressing luciferase and transfected with miRNA mimics were injected intravenously into immunodeficient NOD-SCID mice for 7 days. The experimental group contained 5 animals. The experiments were repeated two times. The total luminescence signal, indicating the engraftment of human cells in the mouse, was analyzed with the Spectral Ami Imaging System (Spectral Instruments Imaging, Tucson, AZ, USA) 24 h after implantation after the injection of luciferin (TriMen Chemicals S.A., Lodz, Poland) at a dose of 150 mg/kg.

Tumors and organs were lysed with a TissueLyser (QIAGEN) and a GeneMATRIX Universal RNA/miRNA Purification Kit (EURx) according to the vendor's protocol. The appearance of RMS cells in the bone marrow 7 days after injection was evaluated by real-time PCR using a human GAPDH-specific primer-probe set (Hs99999905_m1; Applied Biosystems) and compared to murine GAPDH (Mm99999915_g1; Applied Biosystems). Expression of genes and miRNAs was evaluated in tumor samples, as described in Quantitative real-time PCR.

Statistical analysis

Unless otherwise stated, the results are shown as the mean ± standard error of the mean (SEM) of at least 3 independent experiments. Statistical analysis was performed via one-way analysis of variance (ANOVA) with Dunnett's posttest or Student's t test or the Mann-Whitney U test using GraphPad Prism software. Differences with a p value <0.05 were considered statistically significant.

Graphical elements

The graphical abstract was prepared with graphic elements from the Servier Medical Art by Servier, licensed under a Creative Commons Attribution 3.0 Unported License, which allows sharing and adapting items (https://smart.servier.com/).

SUPPLEMENTAL INFORMATION

Supplemental information can be found online at https://doi.org/10.1016/j.omtn.2021.04.013.

ACKNOWLEDGMENTS

We would like to acknowledge Elzbieta Trzyna for validation of STR profile in RH30 cells, Grazyna Drabik for help with histopathological analysis of tumors and Elzbieta Trzesniowska-Popiel for her technical assistance in immunohistochemical staining, Marta Kot for her technical help with flow cytometer, and Grazyna Adamek for her technical help with samples from the experiments *in vivo*. K.S. was a recipient of the Foundation for Polish Science's START scholarship for outstanding young scientists and the Polish Ministry of Science and Higher Education's scholarship for outstanding young scientists. The project was supported by grants from the National Science Centre in Poland to K.S. (2015/17/D/NZ5/02202) and to M.M. (2018/29/B/NZ5/00915 and 2013/09/B/NZ5/00769) and from the Jagiellonian University Medical College to K.S. (N41/DBS/000214).

AUTHOR CONTRIBUTIONS

K.S. conceived the study, designed and coordinated the study, planned and conducted most of the experiments *in vitro* and *in vivo*, analyzed data, performed the statistical analysis, and wrote the manuscript. A.N. participated in the cell culture, the selected western blot analysis, and RNA isolation. B.B. participated in the experiments *in vivo*. M.L. cultured endothelial cells and participated in the adhesion assays. M.M. conceived the study, designed and coordinated the study, and wrote the manuscript. All the authors revised the manuscript.

DECLARATION OF INTERESTS

The authors declare no competing interests.

REFERENCES

1. Skapek, S.X., Ferrari, A., Gupta, A.A., Lupo, P.J., Butler, E., Shipley, J., Barr, F.G., and Hawkins, D.S. (2019). Rhabdomyosarcoma. Nat. Rev. Dis. Primers *5*, 1.
2. Hettmer, S., and Wagers, A.J. (2010). Muscling in: Uncovering the origins of rhabdomyosarcoma. Nat. Med. *16*, 171–173.
3. Cao, L., Yu, Y., Bilke, S., Walker, R.L., Mayeenuddin, L.H., Azorsa, D.O., Yang, F., Pineda, M., Helman, L.J., and Meltzer, P.S. (2010). Genome-wide identification of PAX3-FKHR binding sites in rhabdomyosarcoma reveals candidate target genes important for development and cancer. Cancer Res. *70*, 6497–6508.
4. Szewczyk, B., Skrzypek, K., and Majka, M. (2017). Targeting MET Receptor in Rhabdomyosarcoma: Rationale and Progress. Curr. Drug Targets *18*, 98–107.
5. Skrzypek, K., Kusienicka, A., Szewczyk, B., Adamus, T., Lukasiewicz, E., Miekus, K., and Majka, M. (2015). Constitutive activation of MET signaling impairs myogenic differentiation of rhabdomyosarcoma and promotes its development and progression. Oncotarget *6*, 31378–31398.
6. Skrzypek, K., Kusienicka, A., Trzyna, E., Szewczyk, B., Ulman, A., Konieczny, P., Adamus, T., Badyra, B., Kortylewski, M., and Majka, M. (2018). SNAIL is a key regulator of alveolar rhabdomyosarcoma tumor growth and differentiation through repression of MYF5 and MYOD function. Cell Death Dis. *9*, 643.
7. Skrzypek, K., and Majka, M. (2020). Interplay among SNAIL Transcription Factor, MicroRNAs, Long Non-Coding RNAs, and Circular RNAs in the Regulation of Tumor Growth and Metastasis. Cancers (Basel) *12*, 209.
8. Nieszporek, A., Skrzypek, K., Adamek, G., and Majka, M. (2019). Molecular mechanisms of epithelial to mesenchymal transition in tumor metastasis. Acta Biochim. Pol. *66*, 509–520.
9. Püsküllüoglu, M., Lukasiewicz, E., Miekus, K., Jarocha, D., and Majka, M. (2010). Differential expression of Snail1 transcription factor and Snail1-related genes in alveolar and embryonal rhabdomyosarcoma subtypes. Folia Histochem. Cytobiol. *48*, 671–677.
10. Ulman, A., Skrzypek, K., Konieczny, P., Mussolino, C., Cathomen, T., and Majka, M. (2020). Genome Editing of the *SNAI1* Gene in Rhabdomyosarcoma: A Novel Model for Studies of Its Role. Cells *9*, 1095.
11. Skrzypek, K., Kot, M., Konieczny, P., Nieszporek, A., Kusienicka, A., Lasota, M., Bobela, W., Jankowska, U., Kędracka-Krok, S., and Majka, M. (2020). SNAIL Promotes Metastatic Behavior of Rhabdomyosarcoma by Increasing EZRIN and AKT Expression and Regulating MicroRNA Networks. Cancers (Basel) *12*, 1870.
12. Khordadmehr, M., Shahbazi, R., Sadreddini, S., and Baradaran, B. (2019). miR-193: A new weapon against cancer. J. Cell. Physiol. *234*, 16861–16872.
13. Shirafkan, N., Shomali, N., Kazemi, T., Shanehbandi, D., Ghasabi, M., Baghbani, E., Ganji, M., Khaze, V., Mansoori, B., and Baradaran, B. (2018). microRNA-193a-5p inhibits migration of human HT-29 colon cancer cells via suppression of metastasis pathway. J. Cell. Biochem. *120*, 8775–8783.
14. Yang, Y., Zhou, L., Lu, L., Wang, L., Li, X., Jiang, P., Chan, L.K.Y., Zhang, T., Yu, J., Kwong, J., et al. (2013). A novel miR-193a-5p-YY1-APC regulatory axis in human endometrioid endometrial adenocarcinoma. Oncogene *32*, 3432–3442.
15. Pu, Y., Zhao, F., Cai, W., Meng, X., Li, Y., and Cai, S. (2016). MiR-193a-3p and miR-193a-5p suppress the metastasis of human osteosarcoma cells by down-regulating Rab27B and SRR, respectively. Clin. Exp. Metastasis *33*, 359–372.
16. Girardot, M., Pecquet, C., Chachoua, I., Van Hees, J., Guibert, S., Ferrant, A., Knoops, L., Baxter, E.J., Beer, P.A., Giraudier, S., et al. (2015). Persistent STAT5 activation in myeloid neoplasms recruits p53 into gene regulation. Oncogene *34*, 1323–1332.
17. Almeida, M.I., Nicoloso, M.S., Zeng, L., Ivan, C., Spizzo, R., Gafà, R., Xiao, L., Zhang, X., Vannini, I., Fanini, F., et al. (2012). Strand-specific miR-28-5p and miR-28-3p have distinct effects in colorectal cancer cells. Gastroenterology *142*, 886–896.e9.
18. Zhou, X., Wen, W., Shan, X., Qian, J., Li, H., Jiang, T., Wang, W., Cheng, W., Wang, F., Qi, L., et al. (2016). MiR-28-3p as a potential plasma marker in diagnosis of pulmonary embolism. Thromb. Res. *138*, 91–95.
19. Zhang, L., Pang, Y., Cui, X., Jia, W., Cui, W., Liu, Y., Liu, C., and Li, F. (2019). MicroRNA-410-3p upregulation suppresses proliferation, invasion and migration, and promotes apoptosis in rhabdomyosarcoma cells. Oncol. Lett. *18*, 936–943.
20. Shang, H., Liu, Y., Li, Z., Liu, Q., Cui, W., Zhang, L., Pang, Y., Liu, C., and Li, F. (2019). MicroRNA-874 functions as a tumor suppressor in rhabdomyosarcoma by directly targeting GEFT. Am. J. Cancer Res. *9*, 668–681.
21. Taulli, R., Bersani, F., Foglizzo, V., Linari, A., Vigna, E., Ladanyi, M., Tuschl, T., and Ponzetto, C. (2009). The muscle-specific microRNA miR-206 blocks human rhabdomyosarcoma growth in xenotransplanted mice by promoting myogenic differentiation. J. Clin. Invest. *119*, 2366–2378.
22. Sun, M.M., Li, J.F., Guo, L.L., Xiao, H.T., Dong, L., Wang, F., Huang, F.B., Cao, D., Qin, T., Yin, X.H., et al. (2014). TGF-β1 suppression of microRNA-450b-5p expression: a novel mechanism for blocking myogenic differentiation of rhabdomyosarcoma. Oncogene *33*, 2075–2086.
23. Wang, H., Garzon, R., Sun, H., Ladner, K.J., Singh, R., Dahlman, J., Cheng, A., Hall, B.M., Qualman, S.J., Chandler, D.S., et al. (2008). NF-kappaB-YY1-miR-29 regulatory circuitry in skeletal myogenesis and rhabdomyosarcoma. Cancer Cell *14*, 369–381.
24. Sun, M., Huang, F., Yu, D., Zhang, Y., Xu, H., Zhang, L., Li, L., Dong, L., Guo, L., and Wang, S. (2015). Autoregulatory loop between TGF-β1/miR-411-5p/SPRY4 and MAPK pathway in rhabdomyosarcoma modulates proliferation and differentiation. Cell Death Dis. *6*, e1859.
25. Dmitriev, P., Barat, A., Polesskaya, A., O'Connell, M.J., Robert, T., Dessen, P., Walsh, T.A., Lazar, V., Turki, A., Carnac, G., et al. (2013). Simultaneous miRNA and mRNA transcriptome profiling of human myoblasts reveals a novel set of myogenic differentiation-associated miRNAs and their target genes. BMC Genomics *14*, 265.
26. Hubbard, T., Barker, D., Birney, E., Cameron, G., Chen, Y., Clark, L., Cox, T., Cuff, J., Curwen, V., Down, T., et al. (2002). The Ensembl genome database project. Nucleic Acids Res. *30*, 38–41.
27. Tajsharghi, H., Hammans, S., Lindberg, C., Lossos, A., Clarke, N.F., Mazanti, I., Waddell, L.B., Fellig, Y., Foulds, N., Katifi, H., et al. (2014). Recessive myosin myopathy with external ophthalmoplegia associated with MYH2 mutations. Eur. J. Hum. Genet. *22*, 801–808.
28. Bentzinger, C.F., Wang, Y.X., and Rudnicki, M.A. (2012). Building muscle: molecular regulation of myogenesis. Cold Spring Harb. Perspect. Biol. *4*, a008342.
29. Tsai, K.-W., Leung, C.-M., Lo, Y.-H., Chen, T.-W., Chan, W.-C., Yu, S.-Y., Tu, Y.-T., Lam, H.-C., Li, S.-C., Ger, L.-P., et al. (2016). Arm Selection Preference of MicroRNA-193a Varies in Breast Cancer. Sci. Rep. *6*, 28176.
30. Ory, B., Ramsey, M.R., Wilson, C., Vadysirisack, D.D., Forster, N., Rocco, J.W., Rothenberg, S.M., and Ellisen, L.W. (2011). A microRNA-dependent program controls p53-independent survival and chemosensitivity in human and murine squamous cell carcinoma. J. Clin. Invest. *121*, 809–820.
31. Wang, H., Hertlein, E., Bakkar, N., Sun, H., Acharyya, S., Wang, J., Carathers, M., Davuluri, R., and Guttridge, D.C. (2007). NF-kappaB regulation of YY1 inhibits skeletal myogenesis through transcriptional silencing of myofibrillar genes. Mol. Cell. Biol. *27*, 4374–4387.
32. Yu, T., Li, J., Yan, M., Liu, L., Lin, H., Zhao, F., Sun, L., Zhang, Y., Cui, Y., Zhang, F., et al. (2015). MicroRNA-193a-3p and -5p suppress the metastasis of human non-small-cell lung cancer by downregulating the ERBB4/PIK3R3/mTOR/S6K2 signaling pathway. Oncogene *34*, 413–423.
33. Liu, W., and Wang, X. (2019). Prediction of functional microRNA targets by integrative modeling of microRNA binding and target expression data. Genome Biol. *20*, 18.
34. Agarwal, V., Bell, G.W., Nam, J.W., and Bartel, D.P. (2015). Predicting effective microRNA target sites in mammalian mRNAs. eLife *4*, e05005.
35. Bartolomé-Izquierdo, N., de Yébenes, V.G., Álvarez-Prado, A.F., Mur, S.M., Lopez Del Olmo, J.A., Roa, S., Vazquez, J., and Ramiro, A.R. (2017). miR-28 regulates the germinal center reaction and blocks tumor growth in preclinical models of non-Hodgkin lymphoma. Blood *129*, 2408–2419.
36. Zhu, R.Y., Zhang, D., Zou, H.D., Zuo, X.S., Zhou, Q.S., and Huang, H. (2016). MiR-28 inhibits cardiomyocyte survival through suppressing PDK1/Akt/mTOR signaling. In Vitro Cell. Dev. Biol. Anim. *52*, 1020–1025.
37. Lv, Y., Yang, H., Ma, X., and Wu, G. (2019). Strand-specific miR-28-3p and miR-28-5p have differential effects on nasopharyngeal cancer cells proliferation, apoptosis, migration and invasion. Cancer Cell Int. *19*, 187.

38. Zhu, Z., Wen, Y., Xuan, C., Chen, Q., Xiang, Q., Wang, J., Liu, Y., Luo, L., Zhao, S., Deng, Y., and Zhao, Z. (2020). Identifying the key genes and microRNAs in prostate cancer bone metastasis by bioinformatics analysis. FEBS Open Bio *10*, 674–688.

39. Fazio, S., Berti, G., Russo, F., Evangelista, M., D'Aurizio, R., Mercatanti, A., Pellegrini, M., and Rizzo, M. (2020). The miR-28-5p Targetome Discovery Identified SREBF2 as One of the Mediators of the miR-28-5p Tumor Suppressor Activity in Prostate Cancer Cells. Cells *9*, 354.

40. Ngan, E., Stoletov, K., Smith, H.W., Common, J., Muller, W.J., Lewis, J.D., and Siegel, P.M. (2017). LPP is a Src substrate required for invadopodia formation and efficient breast cancer lung metastasis. Nat. Commun. *8*, 15059.

41. Collet, G., Skrzypek, K., Grillon, C., Matejuk, A., El Hafni-Rahbi, B., Lamerant-Fayel, N., and Kieda, C. (2012). Hypoxia control to normalize pathologic angiogenesis: potential role for endothelial precursor cells and miRNAs regulation. Vascul. Pharmacol. *56*, 252–261.

42. Yi, F., Shang, Y., Li, B., Dai, S., Wu, W., Cheng, L., and Wang, X. (2017). MicroRNA-193-5p modulates angiogenesis through IGF2 in type 2 diabetic cardiomyopathy. Biochem. Biophys. Res. Commun. *491*, 876–882.

43. Takashima, Y., Kawaguchi, A., Iwadate, Y., Hondoh, H., Fukai, J., Kajiwara, K., Hayano, A., and Yamanaka, R. (2019). MicroRNA signature constituted of miR-30d, miR-93, and miR-181b is a promising prognostic marker in primary central nervous system lymphoma. PLoS ONE *14*, e0210400.

44. Fang, L., Ellims, A.H., Moore, X.L., White, D.A., Taylor, A.J., Chin-Dusting, J., and Dart, A.M. (2015). Circulating microRNAs as biomarkers for diffuse myocardial fibrosis in patients with hypertrophic cardiomyopathy. J. Transl. Med. *13*, 314.

45. Roy, S., Benz, F., Vargas Cardenas, D., Vucur, M., Gautheron, J., Schneider, A., Hellerbrand, C., Pottier, N., Alder, J., Tacke, F., et al. (2015). miR-30c and miR-193 are a part of the TGF-β-dependent regulatory network controlling extracellular matrix genes in liver fibrosis. J. Dig. Dis. *16*, 513–524.

46. Heinemann, F.M., Jindra, P.T., Bockmeyer, C.L., Zeuschner, P., Wittig, J., Höflich, H., Eßer, M., Abbas, M., Dieplinger, G., Stolle, K., et al. (2017). Glomerulocapillary miRNA response to HLA-class I antibody in vitro and in vivo. Sci. Rep. *7*, 14554.

47. Toden, S., Zumwalt, T.J., and Goel, A. (2021). Non-coding RNAs and potential therapeutic targeting in cancer. Biochim. Biophys. Acta Rev. Cancer *1875*, 188491.

48. Jarocha, D., Stangel-Wojcikiewicz, K., Basta, A., and Majka, M. (2014). Efficient myoblast expansion for regenerative medicine use. Int. J. Mol. Med. *34*, 83–91.

49. Adamus, T., Konieczny, P., Sekuła, M., Sułkowski, M., and Majka, M. (2014). The strategy of fusion genes construction determines efficient expression of introduced transcription factors. Acta Biochim. Pol. *61*, 773–778.

50. Robinson, J.T., Thorvaldsdóttir, H., Winckler, W., Guttman, M., Lander, E.S., Getz, G., and Mesirov, J.P. (2011). Integrative genomics viewer. Nat. Biotechnol. *29*, 24–26.

51. Rashid, O.M., Nagahashi, M., Ramachandran, S., Dumur, C.I., Schaum, J.C., Yamada, A., Aoyagi, T., Milstien, S., Spiegel, S., and Takabe, K. (2013). Is tail vein injection a relevant breast cancer lung metastasis model? J. Thorac. Dis. *5*, 385–392.